

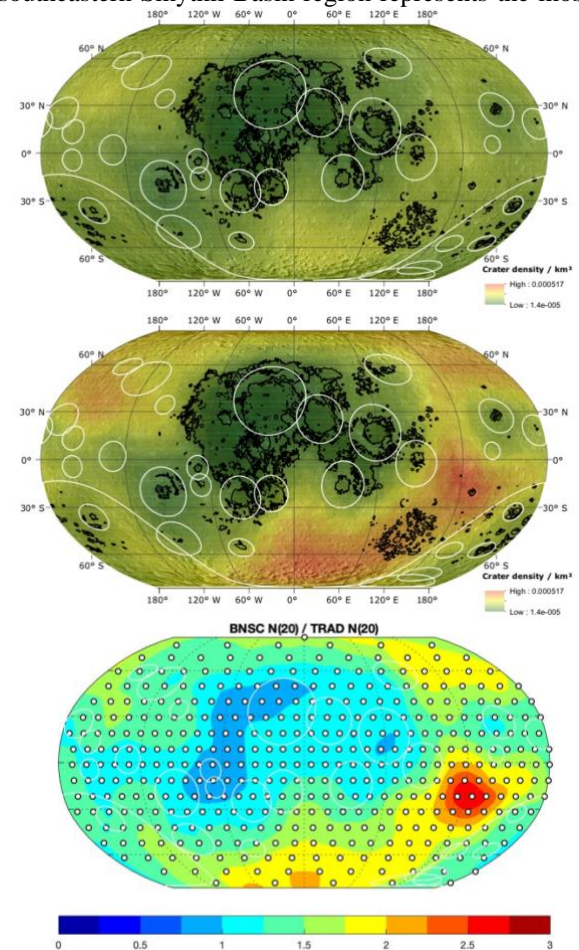
UPDATED LUNAR GLOBAL CRATER DENSITY USING BUFFERED NON-SPARSENESS CORRECTION REVEALS THE OLDEST AGE IN EAST SMYTHII REGION. Y. H. Huang¹, C. Riedel², J. Soderblom¹, S. B. Krein¹, C. Orgel^{3,4}, M. Hirabayashi⁵, D. A. Minton⁶, ¹Department of Earth, Atmospheric, and Planetary Sciences, Massachusetts Institute of Technology, Cambridge, Massachusetts 02139, USA (yahuei@mit.edu), ²Institute of Computer Science, University of Potsdam, Potsdam, Germany 14476, ³Institute of Geological Science, Freie Universität, Berlin, Germany, ⁴European Space Research and Technology Centre (ESA/ESTEC), Noordwijk, The Netherlands, ⁵Department of Aerospace Engineering, Auburn University, Auburn, Alabama 36849 USA, ⁶Department of Earth, Atmospheric, and Planetary Sciences, Purdue University, West Lafayette, Indiana 47907 USA.

Summary of updated lunar crater number density map: We present an updated global density map of all impact craters ≥ 20 kilometers in diameter on the Moon initially produced by Head et al. [1] using the buffered non-sparseness correction technique (BNSC) [2–4]. Figure 1 shows the three maps that highlight the difference in the global lunar crater densities between the traditional crater counting approach (TRAD), similar to Head et al. [1], and the BNSC, as studied in this abstract. In general, younger surfaces such as Procellarum KREEP Terrane and South Pole-Aitken Terrane exhibit similar results for both approaches, while older surfaces, such as the southern nearside and farside highlands exhibit more significant differences with the new approach.

Method: To derive a global lunar crater number density map, we applied the traditional crater counting approach and the buffered non-sparseness correction technique to the lunar crater catalog updated by Kadish et al., [5] from the original catalog by Head et al., [1]. This global lunar catalog counts 5158 craters of ≥ 20 km in diameter. We considered 400 nodes distributed in a quasi equal-area fashion and then determined the surface density of craters ≥ 20 km in diameter by calculating the number density of craters within a radius of 450 km centered on each node. In the final map, the density values represented in each raster cell correspond to the mean crater density value of all overlapping circular reference areas. The traditional crater count approach simply reflects the total number of of all craters that fall within the 450 km-diameter circles (equal crater count area), while the buffered non-sparseness correction technique assigns a new reference area for each individual crater within each node. For a given crater that is evaluated, its new reference area excludes the area of any larger craters and their ejecta [2–4].

Results: We compare the two global lunar crater density maps by rationing the BNSC-derived crater density to the TRAD-derived crater density, allowing us to visualize the difference between the numbers of visible craters and produced craters that the BNSC technique can recover (Figure 1). Currently, the lunar highlands exhibit an excess of ≥ 20 km-diameter craters ≈ 1 –1.5 times the crater density revealed by the TRAD at ≥ 20 km-diameter craters. In a few regions in the

southern nearside and the southeastern PKT region, the number density of ≥ 20 km-diameter craters doubles the estimate by TRAD approach. These areas contain some of the oldest surfaces on the Moon, consistent with the previous findings [1,6]. Most interestingly, the southeastern Smythii Basin region represents the most



excess of ≥ 20 km-diameter craters over a large surface area of 500 km in diameter (red circular area in the bottom panel of Figure 1).

Figure 1: Global lunar crater density map (craters ≥ 20 km in diameter). The top and middle panels represent the map using the traditional crater counting and the buffered non-sparseness correction, while the bottom panel shows the difference of these two approaches in the unit of ratio with color scheme binning into 0.25.

White circles highlight basins with available crater count ages [4]. White data points in the bottom panel show the nodes for calculating crater density. We use Robinson projection.

Implications:

To estimate the absolute model age of the southeastern Smythii Basin region, we fit its cumulative size-frequency distributions from the TRAD and BNSC approaches to the Neukum chronology system [7]. The highest $N(20)$ values in the BNSC for this region are ~ 570 ($4.34^{+0.010}_{-0.011}$ Ga), and its TRAD-derived age is $4.28^{+0.014}_{-0.015}$ Ga. Considering its oldest model crater count age, the southeastern Smythii Basin possesses the geochemical anomaly (e.g., cryptomaria) [8], providing a unique opportunity to examine the geological history of the early Moon for future lunar space exploration missions.

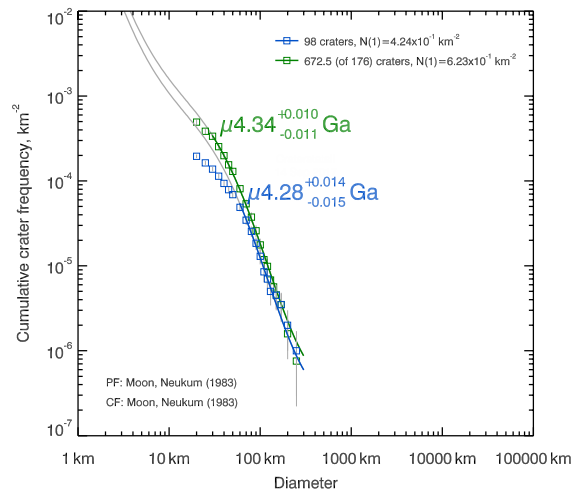


Figure 2: The cumulative size-frequency distributions (CSFD) for the region east of Smythii Basin. Two CSFDs in blue and green represent the distributions from the traditional crater count approach and the BNSC technique. We also fitted both CSFDs to the Neukum chronology system, yielding an absolute model age for this region.

Acknowledgments: This research was supported by Lunar Data Analysis Program grant 80NSSC20K1417.

References: [1] Head, J. et al., *Science* 329, 1504–1507, (2010). [2] Kneissl, T. et al., *Icarus*, 277, 187–195, (2016) [3] Riedel, C. et al., *Earth and Space Science*, 5, 258–267, (2018). [4] Orgel, C. et al. *J. Geophys. Res.: Planets*, 123, 748–762, (2018). [5] Kadish, S. J. et al., *Lunar Planet. Sci. Conf. 42nd* (2011). [6] Povilaitis, R. Z. et al., *Planet. Space Sci.* 162, 41–51 (2018). [7] Neukum, G. et al., *Space Sci. Rev.*, 96, 55–86, (2001). [8] Clark, P. E. and Hawke, B. R. *Earth. Moon. Planets* 53, 93–107 (1991).